Journal of Geosciences, 60 (2015), 1–10 DOI: 10.3190/jgeosci.184

Original paper

Plášilite, $Na(UO_2)(SO_4)(OH)\cdot 2H_2O$, a new uranyl sulfate mineral from the Blue Lizard mine, San Juan County, Utah, USA

Anthony R. KAMPF[1]*, Anatoly V. KASATKIN[2], Jiří ČEJKA[3], Joe MARTY[4]

[1] *Mineral Sciences Department, Natural History Museum of Los Angeles County, 900 Exposition Boulevard, Los Angeles, CA 90007, USA; akampf@nhm.org*
[2] *V/O "Almazjuvelirexport", Ostozhenka str., 22, block 1, 119034 Moscow, Russia*
[3] *Department of Mineralogy and Petrology, National Museum, Cirkusová 1740, 193 00 Prague 9, Czech Republic*
[4] *5199 E. Silver Oak Rd., Salt Lake City, UT 84108, USA*
**Corresponding author*

Plášilite (IMA 2014-021), $Na(UO_2)(SO_4)(OH)\cdot 2H_2O$, is a new uranyl sulfate mineral from the Blue Lizard mine, San Juan County, Utah, USA. The new mineral occurs in and on sandstone matrix in close association with atacamite, blödite, brochantite, calcite, chalcanthite, dickite, gerhardtite, gypsum, hexahydrite, johannite, manganoblödite, natrozippeite and tamarugite. It is a low-temperature, secondary mineral formed by the post-mining weathering of uraninite. Plášilite is monoclinic, with the space group $P2_1/c$, and unit cell parameters a = 8.7122(6), b = 13.8368(4), c = 7.0465(2) Å, β = 112.126(8)°, V = 786.89(7) Å^3 and Z = 4. Crystals are long, thin blades, elongated on [001] and flattened on {100}; rarely occur as prisms, also elongated on [001]. Crystals exhibit the forms {100}, {010} and {011}, and are commonly twinned on {100}. Plášilite is greenish yellow, has a white streak and fluoresces bluish white under both long-wave and short-wave UV. It is transparent with vitreous luster. The mineral has a Mohs hardness probably between 2 and 3, brittle tenacity, even fracture and two perfect cleavages, {010} and {001}. The calculated density based on the empirical formula is 3.726 g/cm^3. The mineral is optically biaxial (+), with α = 1.556(1), β = 1.581(1) and γ = 1.608(1) (measured with white light). The measured 2V is 88(1)° and the calculated 2V is 89°. Dispersion is moderate, $r < v$. The mineral is pleochroic with X = nearly colourless, Y = very pale yellow, Z = pale yellow; $X < Y < Z$. The optical orientation is $X = \mathbf{b}$, $Y \wedge \mathbf{c}$ = 4° in obtuse β. The empirical formula of plášilite is $Na_{0.94}(UO_2)(S_{1.01}O_4)(OH)(H_2O)_2$ (based on 9 O *apfu*). Prominent features in the Raman spectrum include the symmetric stretching vibrations of the uranyl (UO_2^{2+}) group and sulfate tetrahedra and the O–H stretching and bending vibrations of the H_2O molecules. The eight strongest powder X-ray diffraction lines are [d_{obs} Å(I)(hkl)]: 6.90(100)(020), 5.85(99)(011,$\bar{1}11$), 4.024(57)(200,130), 3.492(82) ($\bar{1}02$,220,040), 3.136(40)($\bar{1}22$), 2.690(25)(141,102,$\bar{2}41$,032), 2.618(34)(240,150,$\bar{3}02$), 1.9212(30)(mult.). The crystal structure of plášilite (R_1 = 0.019 for 1603 reflections with $F_{obs} > 4\sigma F$) contains uranyl sulfate sheets of composition $[(UO_2)_2(SO_4)_2(OH)_2]^{2-}$ parallel to (010). Between the sheets and linking them to one another are chains of edge-sharing $NaO_2(H_2O)_4$ octahedra parallel to [001]. The uranyl sulfate sheet is based on the phosphuranylite anion topology. The sheets in plášilite and deliensite are geometrical isomers.

Keywords: plášilite, new mineral, crystal structure, Raman spectroscopy, uranyl sulfate, Blue Lizard mine
Received: 25 June 2014; accepted: 23 November 2014; handling editor: F. Laufek
The online version of this article (doi: 10.3190/jgeosci.184) contains supplementary electronic material.

1. Introduction

Uranyl sulfate minerals typically form by hydration–oxidation weathering of primary uranium minerals, mainly uraninite, by acidic solutions derived from the decomposition of associated sulfides (Finch and Murakami 1999; Krivovichev and Plášil 2013). They are found in most uranium deposits world-wide.

Our mineralogical investigations of the Blue Lizard mine over the last few years have revealed a remarkable secondary assemblage of uranyl sulfates, the majority of which are new to science. We have already described the sodium uranyl sulfates meisserite (Plášil et al. 2013), bluelizardite (Plášil et al. 2014a) and belakovskiite (Kampf et al. 2014), and herein we introduce plášilite, the fourth new sodium uranyl sulfate. In addition, six other new uranyl sulfates from this mine, are currently under study and all, except one, contain essential Na.

The discovery of such a wealth of new uranyl sulfates at a single mine is unprecedented. The classic Jáchymov deposit has yielded more uranyl sulfates (Ondruš et al. 1997; Tvrdý and Plášil 2010); however, they have been described from several mines and over a lengthy time period. Furthermore, it is remarkable that seven of the ten new phases from the Blue Lizard mine feature only Na as the additional cation and only one contains no essential Na. The only sodium uranyl sulfate mineral known previously was natrozippeite (Frondel et al. 1976).

Plášilite (‘pla: shil ait) is named for Jakub Plášil (born 1984), a researcher in the Department of Structure Analysis at the Institute of Physics, Academy of Sciences of the Czech Republic. His scientific research is focused on the crystal chemistry of hydrated oxysalts and hexavalent uranium compounds. He is author or co-author of more than 80 publications, including the descriptions of 23 new mineral species.

The new mineral and the name were approved by the Commission on New Minerals, Nomenclature and Classification of the International Mineralogical Association (IMA2014-021). The description is based on six cotype specimens. Five of them are deposited in the collections of the Natural History Museum of Los Angeles County, catalogue numbers 64126, 64127, 64128, 64129 and 64130. A sixth cotype specimen is housed in the collections of the Fersman Mineralogical Museum of the Russian Academy of Sciences, Moscow, Russia, registration number 4548/1. Crystals from that specimen were used for the chemical analyses.

2. Occurrence

Plášilite was found underground in the Blue Lizard Mine, Red Canyon, White Canyon District, San Juan County, Utah, USA (37°33'26"N 110°17'44"W) by one of the authors (JM). The Blue Lizard mine is located *c.* 72 km west of the town of Blanding, Utah, and *c.* 22 km southeast of Good Hope Bay on Lake Powell. It is on the northern side of Red Canyon and close to the Markey mine. Information on the history and geology of the deposit is taken largely from Chenoweth (1993).

The deposit was first recognized in the summer of 1898 by John Wetherill, while leading an archeological expedition into Red Canyon. He noted yellow stains around a petrified tree. At that spot, he built a rock monument, in which he placed a piece of paper to claim the minerals. Although he never officially recorded his claim, 45 years later, in 1943, he described the spot to Preston V. Redd of Blanding, Utah, who went to the site, found Wetherill’s monument and claimed the area as the Blue Lizzard claim (note alternate spelling). Underground workings to mine uranium were not developed until the 1950s.

Mineralized channels are found in the Shinarump Member of the Chinle Fm. The Shinarump Member consists of medium- to coarse-grained sandstone, conglomeratic sandstone beds and thick siltstone lenses. Ore minerals were deposited as replacements of wood and other organic material and as disseminations in the enclosing sandstone. Since the mine closed in 1978, oxidation of primary ores in the humid underground environment has produced a variety of secondary minerals, mainly sulfates, as efflorescent crusts on the surfaces of mine walls.

Plášilite is a relatively widespread mineral in the secondary uranyl sulfate mineral assemblages at the Blue Lizard mine. Other secondary minerals found in direct association with plášilite include atacamite, blödite, brochantite, calcite, chalcanthite, dickite, gerhardtite, gypsum, hexahydrite, johannite, manganoblödite, natrozippeite and tamarugite. Primary quartz (sandstone) comprises the bulk of the matrix. Additional primary minerals include baryte, bornite, chalcopyrite, covellite, feldspar, pyrite and uraninite. Other secondary minerals in the general assemblage include belakovskiite, bluelizardite, boyleite, cobaltoblödite, copiapite, coquimbite, cyanotrichite, d’ansite-(Mn), deliensite, ferrinatrite, halite, kröhnkite, lishizhenite, meisserite, metavoltine, pickeringite, pseudojohannite, rhomboclase, römerite and sideronatrite.

Plášilite has formed late in the secondary uranyl sulfate mineral assemblages. Of the associated phases noted above, only hexahydrite has been observed growing on plášilite. Crystals of plášilite placed upon damp pH paper provide a pH between 2 and 3, indicative of strongly to moderately acidic conditions during the formation of the mineral.

3. Physical and optical properties

Plášilite occurs as long, thin blades (Fig. 1), elongated on [001] and flattened on {100}; rarely as prisms (Fig. 2), also elongated on [001]. Crystals exhibit the forms {100}, {010} and {011} (Fig. 3). Twinning is common on {100}; prismatic crystals show polysynthetic twinning. Plášilite is greenish yellow, has a white streak and fluoresces bluish white under both long-wave and short-wave UV. It is transparent with vitreous lustre. The Mohs hardness could not be measured, but is probably between 2 and 3, based upon the

Tab. 1 Gladstone-Dale compatibilities of recently-described uranyl sulfate minerals

Mineral	Reference	Ideal formula	n_{av}	Compatibility Larsen*	Compatibility Mandarino**
belakovskiite	Kampf et al. (2014)	$Na_7(UO_2)(SO_4)_4(SO_3OH)\cdot3H_2O$	1.5113	0.023	–0.005
beshtauite	Pekov et al. (2013)	$(NH_4)_2(UO_2)(SO_4)_2\cdot2H_2O$	1.5747	0.044	0.000
bluelizardite	Plášil et al. (2014a)	$Na_7(UO_2)(SO_4)_4Cl\cdot2H_2O$	1.5333	0.033	0.005
mathesiusite	Plášil et al. (2014b)	$K_5(UO_2)_4(SO_4)_4(VO_5)\cdot4H_2O$	1.6217	0.070	0.011
meisserite	Plášil et al. (2013)	$Na_4(UO_2)(SO_4)_4\cdot2H_2O$	1.5390	0.018	–0.015
plášilite	This study	$Na(UO_2)(SO_4)(OH)\cdot2H_2O$	1.5817	0.063	0.000

based upon empirical formulae for $k(UO_3)$ = 0.134 (*Larsen 1921) and $k(UO_3)$ = 0.118 (**Mandarino 1976)

Fig. 1 Sprays of plášilite blades with tamarugite (white) on blödite and quartz. FOV 3 mm wide.

behavior of crystals when broken. The mineral exhibits brittle tenacity, even fracture and two perfect cleavages, {010} and {001}. The mineral is easily soluble in room-temperature H_2O. The density was not measured because plášilite is soluble in Clerici solution. The calculated density based on the empirical formula is 3.726 g/cm^3.

The mineral is optically biaxial (+), with $\alpha = 1.556(1)$, $\beta = 1.581(1)$ and $\gamma = 1.608(1)$ (measured with white light). The 2*V* obtained by direct conoscopic observation using a spindle stage is 88(1)° and the calculated 2*V* is 89°. Dispersion is moderate, $r < v$. The mineral is pleochroic with X = nearly colorless, Y = very pale yellow, Z = pale yellow; $X < Y < Z$. The optical orientation is $X = \mathbf{b}$, $Y \wedge \mathbf{c} = 4°$ in obtuse β.

The Gladstone-Dale compatibility, $1 - (K_p/K_c)$, is 0.0004 for the empirical formula and 0.0029 for the ideal formula, in both cases in the range of superior compatibility. Note that the compatibility was calculated using $k(UO_3) = 0.118$ (Mandarino 1976), rather than $k(UO_3) = 0.134$, the value originally given by Larsen (1921). Piret and Deliens (1989) recommended the latter value for uranyl phosphates and arsenates and Mandarino (1994) did so for selenites and selenates; however, for uranyl sulfates, $k(UO_3) = 0.118$ provides far better compatibilities (See Tab. 1).

4. Chemical composition

The chemical composition of plášilite was determined using a CamScan4D scanning electron microscope

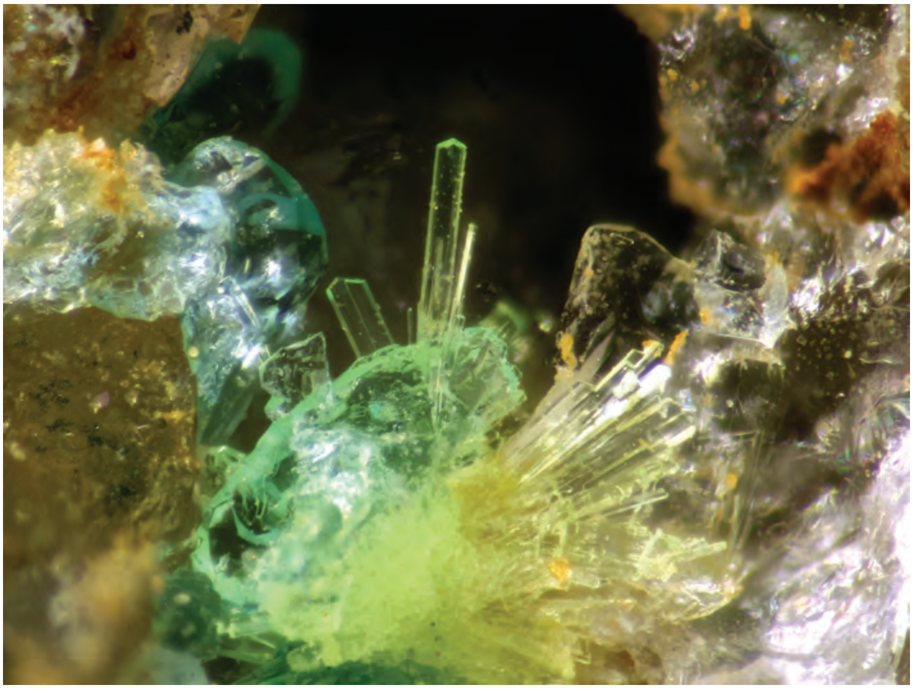

Fig. 2 Plášilite blades with chalcanthite on quartz. FOV 1.8 mm.

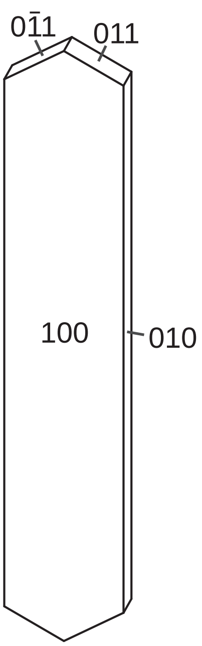

Fig. 3 Crystal drawing of plášilite; clinographic projection in standard orientation.

(SEM) equipped with an Oxford Link ISIS energy-dispersive X-ray spectrometer. An operating voltage of 20 kV was used with a beam current of 1 nA and a 1 µm beam diameter. The EDS mode on the SEM was chosen for the analysis instead of the WDS mode on the electron microprobe because of the instability of plášilite under the electron beam caused by high contents of both Na and H_2O. Attempts to use the WDS mode were unsuccessful due to rapid and significant decomposition of the mineral under the electron beam. Although plášilite is a relatively widespread mineral in the secondary uranyl sulfate mineral assemblages at the Blue Lizard mine, it is present in very small quantities, making it impossible to separate an adequate amount of pure material for direct determination of H_2O. Consequently, H_2O was calculated by stoichiometry on the basis of 9 O *apfu* as indicated by the crystal structure determination. Raman spectroscopy confirmed the absence of CO_2 and the presence of H_2O and OH in the mineral. Other than U, Na and S, no elements with atomic numbers higher than 8 were observed. Nine spot analyses provided the data reported in Tab. 2.

Tab. 2 Analytical data for plášilite (wt. %)

Constituent	Mean (*n* = 9)	Range	SD	Probe standard
Na_2O	6.61	5.42–7.63	0.59	Chkalovite
UO_3	65.15	64.47–66.30	0.60	UO_2
SO_3	18.33	17.63–19.19	0.45	ZnS
H_2O	10.24*			
Total	100.33			

* calculated from structure
SD – standard deviation

The empirical formula of plášilite, calculated on the basis of 9 O *apfu*, is $Na_{0.94}(UO_2)(S_{1.01}O_4)(OH)(H_2O)_2$. The ideal formula is $Na(UO_2)(SO_4)(OH)\cdot 2H_2O$, which requires (in wt. %) Na_2O 7.01, UO_3 64.70, SO_3 18.11 and H_2O 10.19, total 100.

5. Raman spectroscopy

A Raman spectrum (Fig. 4) of plášilite crystal was collected using a DXR dispersive Raman spectrometer (Thermo Scientific) mounted on a confocal Olympus microscope (100× objective). The Raman signal was excited by a 532 nm diode-pumped solid-state laser and detected by a CCD detector. The experimental parameters were: 5s exposure time; 32 exposures, 400 lines/mm grating, 25 micron pinhole spectrograph aperture and 3.0 mW laser power level. The instrument was calibrated by a software-controlled calibration procedure using multiple neon emission lines (wavelength calibration), multiple polystyrene Raman bands (laser frequency calibration) and standardized white light sources (intensity calibration).

The foregoing interpretation of the Raman spectrum of plášilite is based upon Nakamoto (1986), Volod'ko et al. (1981) and Čejka (1999, 2004, 2007). The crystal structure of plášilite contains one symmetrically distinct U^{6+}, one symmetrically distinct S^{6+} and one symmetrically distinct Na^+. The free uranyl ion, $(UO_2)^{2+}$ with the point symmetry $D_{\alpha h}$, exhibits three fundamental modes: the ν_1 (Σ_g^+) symmetric stretching vibration, Raman active at 900–750 cm^{-1}, the ν_2 (δ) (Π_u) doubly degenerate bending vibration, infrared active at 300–200 cm^{-1}, and the ν_3 (Σ_u) antisymmetric stretching vibration, infrared active at 1000–850 cm^{-1}. The symmetry decrease from $D_{\alpha h}$ to $C_{\alpha v}$ or C_{2v} may cause the infrared activation of the ν_1 vibration, Raman activation of the ν_2 and ν_3 vibrations as well as splitting of the ν_2 doubly degenerate bending vibration. Sulfate anion, $(SO_4)^{2-}$, in T_d symmetry, exhibits four fundamental modes: the ν_1 (A_1) symmetric stretching vibration, Raman active at ~983 cm^{-1}, the ν_2 (δ) (*E*) doubly degenerate bending vibration, Raman active at ~450 cm^{-1}, the ν_3 (F_2) triply degenerate antisymmetric stretching vibration, infrared and Raman active at ~1105 cm^{-1}, and the ν_4 (δ) (F_2) triply degenerate bending vibration, infrared and Raman active at ~611 cm^{-1}.

A band at 3600 cm^{-1} was assigned to the ν(OH) stretching vibration of free or weakly hydrogen-bonded hydroxyl ions. Bands at 3530 and 3385 cm^{-1} are attributed to the ν(OH) stretching vibrations of structurally nonequivalent hydrogen bonded water molecules. According to Libowitzky (1999),

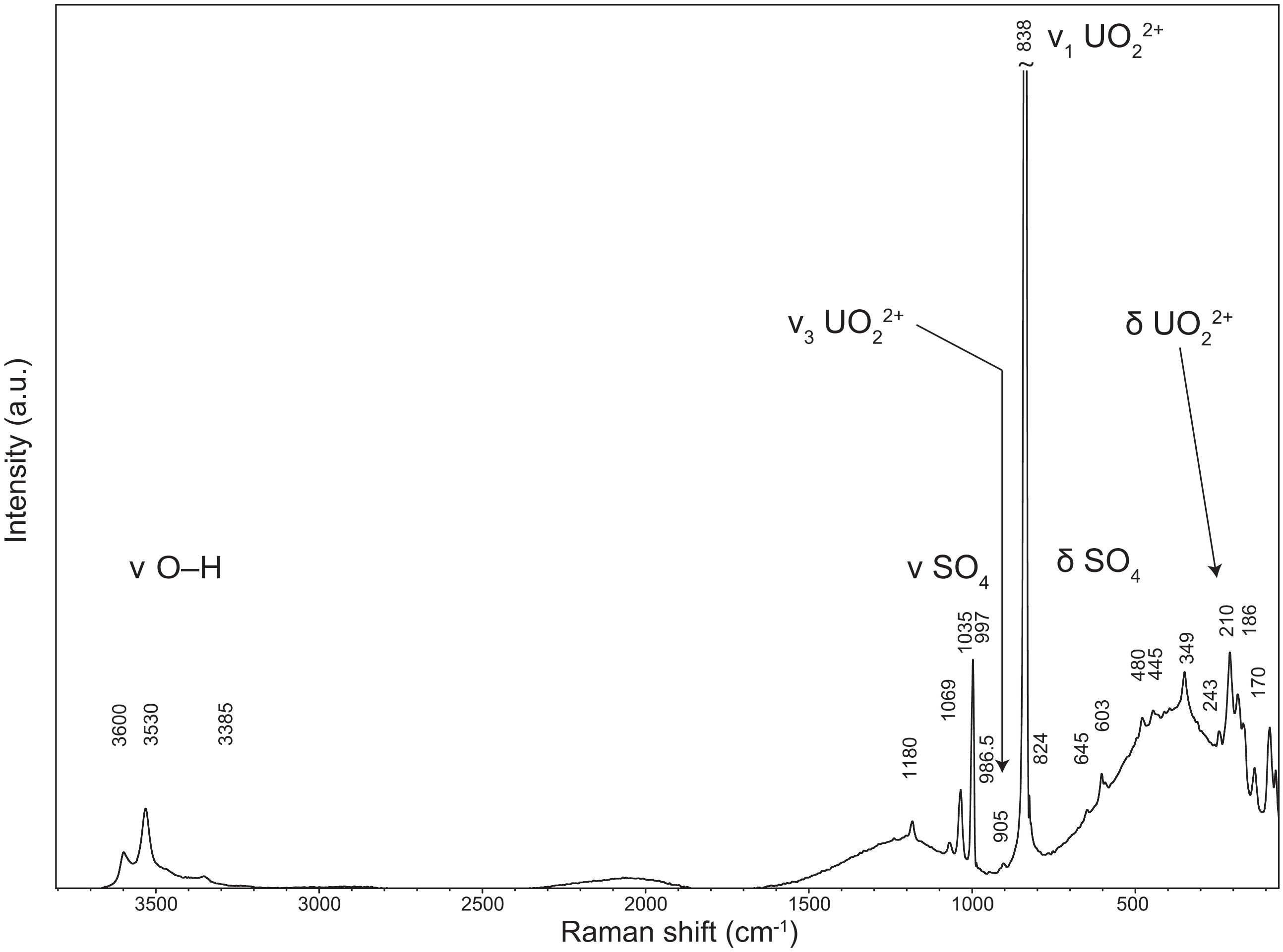

Fig. 4 The Raman spectrum of plášilite.

approximate O–H···O hydrogen bond lengths are > 3.2 Å/3599 cm^{-1}, 2.96 Å/3532 cm^{-1} and 2.79 Å/3385 cm^{-1}. No bands were observed in the region of bending vibrations of water molecules (~1600 cm^{-1}).

Bands at 1180, 1069 and 1035 cm^{-1} are assigned to the split triply degenerate $\nu_3(SO_4)^{2-}$ antisymmetric stretching vibrations and a strong band at 997 cm^{-1} to the $\nu_1(SO_4)^{2-}$ symmetric stretching vibration. A shoulder at 986.5 cm^{-1} may be assigned to the δU–OH bending vibration or the $\nu_1(SO_4)^{2-}$ vibration.

A weak band at 905 cm^{-1} is connected with the $\nu_3(UO_2)^{2+}$ antisymmetric stretching vibration. A very strong band at 838 cm^{-1} was attributed to the $\nu_1(UO_2)^{2+}$ symmetric stretching vibration, while a shoulder at 824 cm^{-1} may be assigned to the same vibration or to the δ U–OH bending vibration. According to Bartlett and Cooney (1989), approximate U–O bond lengths in the uranyl ion are 1.78 Å/904 cm^{-1}, 1.78 Å/838 cm^{-1} and 1.79 Å/824 cm^{-1}. All these U–O bond lengths are close to those inferred by Burns (2005) for uranyl pentagonal dipyramidal coordination polyhedra and agree with U–O bond lengths in the plášilite structure determined by X-ray diffraction.

Bands at 645 and 603 cm^{-1} are connected with triply degenerate $\nu_4(\delta)(SO_4)^{2-}$ bending vibrations, and bands at 480 and 445 cm^{-1} to the doubly degenerate $\nu_2(\delta)(SO_4)^{2-}$ bending vibrations. A band at 349 cm^{-1} may probably be assigned to $\nu(U–O_{equatorial})$ stretching vibrations. The doubly degenerate $\nu_2(\delta)(UO_2)^{2+}$ bending vibration is characterized by a band at 243 cm^{-1}. Remaining bands at 210, 186, 170, 137, 88 and 70 cm^{-1} may be assigned to lattice modes.

6. X-ray crystallography and structure determination

6.1. Powder diffraction

Powder X-ray diffraction data for plášilite were obtained using a Rigaku R-Axis Rapid II curved imaging plate microdiffractometer utilizing monochromatized MoK_α radiation (Gandolfi method). Observed powder d_{hkl} values and intensities were derived by profile fitting using JADE 2010 software (Materials Data Inc.). Data (in Å)

Tab. 3 Powder X-ray diffraction data for plášilite

I_{obs}	d_{obs}	d_{calc}	I_{calc}	*h k l*
100	6.90	6.9184	100	0 2 0
99	5.85	5.9036	42	0 1 1
		5.7981	42	$\bar{1}$ 1 1
15	4.72	4.7479	7	0 2 1
		4.6924	8	$\bar{1}$ 2 1
		4.1400	6	1 1 1
57	4.024	4.0353	37	2 0 0
		4.0045	23	1 3 0
21	3.731	3.7668	8	0 3 1
		3.7390	8	$\bar{1}$ 3 1
		3.6757	4	1 2 1
		3.5997	6	$\bar{2}$ 2 1
82	3.492	3.5217	27	$\bar{1}$ 0 2
		3.4857	34	2 2 0
		3.4592	20	0 4 0
40	3.136	3.1385	33	$\bar{1}$ 2 2
		3.1115	2	$\bar{2}$ 3 1
9	3.050	3.0565	6	0 4 1
		3.0416	4	$\bar{1}$ 4 1
14	2.898	2.9025	17	2 1 1
13	2.841	2.8401	15	$\bar{3}$ 1 1
25	2.690	2.7048	4	1 4 1
		2.6936	18	1 0 2
		2.6740	3	$\bar{2}$ 4 1
		2.6642	2	0 3 2
34	2.618	2.6263	8	2 4 0
		2.6177	7	1 5 0
		2.6148	16	$\bar{3}$ 0 2
		2.5392	2	$\bar{1}$ 5 1
14	2.509	2.5101	9	1 2 2
		2.4962	5	2 3 1
		2.4678	5	$\bar{1}$ 4 2
18	2.457	2.4562	7	$\bar{3}$ 3 1
		2.4459	7	$\bar{3}$ 2 2
		2.3238	4	3 3 0
10	2.293	2.3008	4	$\bar{1}$ 1 3
		2.2818	5	$\bar{2}$ 1 3
		2.2110	3	$\bar{1}$ 2 3
15	2.173	2.1834	2	3 1 1
		2.1744	5	0 6 1
		2.1690	6	$\bar{1}$ 6 1
		2.1494	4	0 1 3
14	2.122	2.1253	7	1 4 2
		2.1107	3	0 5 2
		2.1062	2	3 2 1
		2.1038	3	$\bar{3}$ 1 3
20	2.084	2.0912	3	$\bar{2}$ 5 2
		2.0859	7	$\bar{3}$ 4 2
		2.0725	2	$\bar{4}$ 2 1
		2.0679	2	$\bar{2}$ 3 3
18	2.021	2.0364	4	1 6 1
		2.0242	2	2 5 1
		2.0231	6	$\bar{2}$ 6 1
		2.0177	5	4 0 0
		2.0027	2	$\bar{3}$ 5 1
5	1.9620	1.9679	2	0 3 3
		1.9631	3	2 3 2
30	1.9212	1.9370	4	4 2 0
		1.9344	3	$\bar{1}$ 4 3
		1.9290	6	3 5 0
		1.9230	2	$\bar{2}$ 4 3
		1.9199	9	1 7 0
		1.9169	3	$\bar{4}$ 3 2
		1.9080	5	1 1 3
11	1.8538	1.8630	4	3 4 1
		1.8553	6	$\bar{4}$ 1 3
		1.8396	3	$\bar{4}$ 4 1
3	1.8195	1.8212	2	2 6 1
		1.8129	2	$\bar{3}$ 4 3
8	1.7667	1.7776	3	1 3 3
		1.7738	3	3 0 2
		1.7608	6	$\bar{2}$ 0 4
11	1.7350	1.7429	3	4 4 0
		1.7367	5	4 1 1
		1.7348	3	$\bar{4}$ 3 3
		1.7285	2	$\bar{5}$ 0 2
13	1.7088	1.7182	3	3 2 2
		1.7124	6	$\bar{5}$ 1 1
		1.7073	2	2 5 2
		1.7064	4	$\bar{2}$ 2 4
		1.6908	5	0 7 2
14	1.6771	1.6807	5	$\bar{2}$ 7 2
		1.6769	4	$\bar{5}$ 2 2
		1.6719	2	0 8 1
		1.6694	2	$\bar{1}$ 8 1
13	1.6315	1.6402	4	$\bar{1}$ 6 3
		1.6367	3	4 3 1
		1.6333	2	$\bar{2}$ 6 3
		1.6319	3	0 0 4
		1.6163	3	$\bar{5}$ 3 1
20	1.5925	1.6066	2	1 8 1
		1.6001	3	$\bar{2}$ 8 1
		1.5960	5	3 6 1
		1.5929	4	3 7 0
		1.5883	3	0 2 4
		1.5826	2	0 6 3
		1.5812	4	$\bar{4}$ 6 1
		1.5784	2	3 4 2
9	1.5653	1.5692	3	$\bar{2}$ 4 4
		1.5641	2	$\bar{3}$ 6 3
		1.5556	3	$\bar{4}$ 2 4
2	1.5056	1.5103	3	1 9 0
6	1.4669	1.4679	2	$\bar{5}$ 4 3
		1.4611	4	2 7 2
5	1.4459	1.4495	2	$\bar{4}$ 4 4
		1.4418	3	$\bar{4}$ 7 2
		1.4384	2	3 1 3
9	1.3874	1.3979	2	$\bar{6}$ 1 3
		1.3908	2	0 9 2
		1.3852	3	$\bar{2}$ 9 2

Only calculated lines with $I_{calc} \geq 2$ are shown

are given in Tab. 3. Unit-cell parameters refined from the powder data with whole-pattern fitting are: *a* = 8.697(2), *b* = 13.827(2), *c* = 7.065(2) Å, β = 112.118(7)° and *V* = 787.1(3) Å^3.

6.2. Single-crystal X-ray diffraction and structure solution

Single-crystal data for plášilite were collected on a Rigaku R-Axis Rapid II curved imaging plate microdiffractometer using monochromatized MoK_α radiation. The CrystalClear software package (Rigaku Corp.) was employed for processing structure data, including the application of an empirical multi-scan absorption correction using ABSCOR (Higashi 2001). The structure was solved by direct methods using SIR2004 (Burla et al. 2005). SHELXL-2013 (Sheldrick 2008) was utilized for the refinement of the structure. A difference Fourier synthesis located all H atom positions, which were then refined with soft restraints of 0.82(3) Å on the O–H distances and 1.30(3) Å on the H–H distances and with the U_{eq} of each H set to 1.2 times that of the donor O atom. Data collection and refinement details are given in Tab. 4, atom coordinates and displacement parameters in Tab. 5, selected bond distances in Tab. 6, and a bond-valence analysis in Tab. 7.

6.3. Description of the crystal structure

The U site in the structure of plášilite is surrounded by seven O atom sites forming a squat pentagonal bipyramid. This is a typical coordination for U^{6+} in which the two short apical bonds of the bipyramid constitute the uranyl group. The observed uranyl bond-lengths in plášilite (U–O5 = 1.779 and U–O6 = 1.781Å; Tab 5) closely match the typical value for the uranyl bond-length given by Burns et al. (1997), based on a large-number of well-refined crystal structures. In the structure, pairs of pentagonal bipyramids share a common edge, forming dimers. The dimers are linked by sharing corners with SO_4 groups, yielding a $[(UO_2)_2(SO_4)_2(OH)_2]^{2-}$ sheet parallel to (010) (Fig. 5). Between the sheets are $NaO_2(H_2O)_4$ octahedra, which link by sharing *trans* H_2O–H_2O edges to form chains along [001]. Sodium octahedra link the sheets in the [010] direction; each Na octahedron shares one O corner with an SO_4 group in the sheet and the opposite O corner with a uranyl group. The framework thereby created is further linked via relatively weak hydrogen bonds (Fig. 6).

The $[(UO_2)_2(SO_4)_2(OH)_2]^{2-}$ sheet is based on the phosphuranylite anion topology (Burns 2005), with a ring symbol $6^15^24^23^2$ (Krivovichev and Burns 2007). The sheets in johannite, $Cu[(UO_2)_2(OH)_2(SO_4)_2](H_2O)_8$, (Mereiter 1982) and deliensite, $Fe(UO_2)_2(SO_4)_2(OH)_2\cdot 7H_2O$, (Plášil et al. 2012) are topologically identical to that in plášilite; however, the sheets are geometrical isomers, differing in the orientation of the SO_4 groups (Fig. 5). It is worth noting that plášilite and johannite occur in direct association at the Blue Lizard mine, and deliensite has been found in the general assemblage. None of the other uranyl sulfates recorded at the Blue Lizard mine (e.g. belakovskiite, bluelizardite, meisserite and several

Tab. 4 Data collection and structure refinement details for plášilite

Temperature	298(2) K
Structural formula	$Na(UO_2)(SO_4)(OH)(H_2O)_2$
Space group	$P2_1/c$
Unit-cell dimensions	a = 8.7122(6) Å
	b = 13.8368(4) Å
	c = 7.04650(17) Å
	β = 112.126(8)°
V	786.89(7) Å^3
Z	4
Density (for above formula)	3.723 g cm^{-3}
Absorption coefficient	20.965 mm^{-1}
F(000)	780
Crystal size	80 × 20 × 5 μm
θ range	3.45 to 27.48°
Index ranges	$-11 \leq h \leq 11$, $-15 \leq k \leq 17$, $-7 \leq l \leq 9$
Reflections collected/unique	7709/1794; R_{int} = 0.0295
Reflections with $F_o > 4\sigma(F)$	1609
Completeness to θ = 27.48°	99.4%
Refinement method	Full-matrix least-squares on F^2
Parameters refined	124
GoF	1.081
Final R indices [$F_o > 4\sigma(F)$]	R_1 = 0.0194, wR_2 = 0.0446
R indices (all data)	R_1 = 0.0231, wR_2 = 0.0462
Largest diff. peak/hole	+3.07/–0.70 e A^{-3}

*$R_{int} = \Sigma|F_o^2 - F_o^2(\text{mean})|/\Sigma[F_o^2]$. GoF = $S = \{\Sigma[w(F_o^2 - F_c^2)^2]/(n-p)\}^{1/2}$. $R_1 = \Sigma||F_o| - |F_c||/\Sigma|F_o|$. $wR_2 = \{\Sigma[w(F_o^2 - F_c^2)^2]/\Sigma[w(F_o^2)^2]\}^{1/2}$; $w = 1/[\sigma^2(F_o^2) + (aP)^2 + bP]$ where a is 0.026, b is 0.4537 and P is $[2F_c^2 + \text{Max}(F_o^2,0)]/3$.

Tab. 5 Atom coordinates and displacement parameters (Å^2) for plášilite

	x/a	*y/b*	*z/c*	U_{eq}	U_{11}	U_{22}	U_{33}	U_{23}	U_{13}	U_{12}
U	0.23417(2)	0.46715(2)	0.12219(2)	0.01131(7)	0.00812(10)	0.01565(10)	0.00985(10)	–0.00007(5)	0.00306(6)	0.00043(6)
S	0.32042(13)	0.50289(8)	0.66758(15)	0.01204(19)	0.0089(5)	0.0173(5)	0.0097(5)	0.0013(4)	0.0033(4)	0.0011(4)
Na	0.2793(3)	0.73085(15)	0.6584(3)	0.0305(5)	0.0401(12)	0.0251(10)	0.0272(10)	–0.0035(8)	0.0136(9)	0.0062(9)
O1	0.1796(4)	0.5684(2)	0.6139(5)	0.0187(6)	0.0107(15)	0.0222(15)	0.0231(16)	0.0033(13)	0.0062(12)	0.0038(13)
O2	0.3124(4)	0.4419(2)	0.4914(4)	0.0205(7)	0.0261(18)	0.0238(16)	0.0104(15)	–0.0004(12)	0.0055(13)	0.0040(14)
O3	0.4736(4)	0.5623(2)	0.7334(5)	0.0186(6)	0.0076(15)	0.0242(15)	0.0208(16)	0.0025(13)	0.0018(12)	0.0012(12)
O4	0.3242(4)	0.4368(2)	0.8366(4)	0.0173(6)	0.0236(17)	0.0207(15)	0.0099(14)	0.0047(12)	0.0090(13)	0.0065(13)
O5	0.1933(4)	0.3410(2)	0.1168(4)	0.0229(7)	0.0236(18)	0.0204(16)	0.0229(17)	–0.0032(13)	0.0069(14)	0.0072(14)
O6	0.2856(4)	0.5921(2)	0.1325(5)	0.0225(7)	0.0179(16)	0.0186(16)	0.0309(18)	–0.0006(13)	0.0092(14)	0.0015(13)
OH7	–0.0008(4)	0.5113(3)	0.1785(5)	0.0240(7)	0.0120(16)	0.048(2)	0.0127(16)	0.0048(15)	0.0053(13)	0.0057(15)
H7	–0.002(8)	0.483(4)	0.276(7)	0.029						
OW8	–0.0797(5)	0.2716(3)	0.6917(6)	0.0326(8)	0.028(2)	0.034(2)	0.035(2)	–0.0005(18)	0.0121(16)	0.0040(16)
H8A	0.006(5)	0.242(3)	0.702(9)	0.039						
H8B	–0.044(7)	0.328(2)	0.719(9)	0.039						
OW9	0.5186(5)	0.2503(3)	0.0025(6)	0.0319(8)	0.033(2)	0.0272(18)	0.034(2)	–0.0076(17)	0.0115(16)	0.0021(17)
H9A	0.475(7)	0.296(3)	–0.063(8)	0.038						
H9B	0.448(6)	0.210(3)	–0.020(8)	0.038						

Tab. 6 Selected bond distances (Å) and angles (°) for plášilite

U–O5	1.779(3)	Na–O1	2.387(4)	S–O1	1.456(3)	Hydrogen bonds (D = donor, A = acceptor)						
U–O6	1.781(3)	Na–OW9	2.389(4)	S–O2	1.481(3)	D–H	d(D–H)	d(H···A)	<DHA	d(D···A)	A	<HDH
U–OH7	2.310(3)	Na–OW8	2.417(4)	S–O3	1.485(3)	OH7–H7	0.80(3)	2.10(5)	137(6)	2.739(5)	O1	
U–OH7	2.338(3)	Na–OW8	2.425(4)	S–O4	1.492(3)	OW8–H8a	0.82(3)	2.26(3)	161(5)	3.050(5)	O5	
U–O3	2.394(3)	Na–OW9	2.442(4)	<S–O>	1.479	OW8–H8b	0.84(3)	2.32(3)	166(5)	3.141(5)	O7	101
U–O2	2.454(3)	Na–O6	2.459(4)			OW9–H9a	0.79(3)	2.31(3)	162(6)	3.066(5)	O4	
U–O4	2.456(3)	<Na–O>	2.420			OW9–H9b	0.80(3)	2.43(3)	161(5)	3.193(5)	O2	120
<U–O>	2.289											

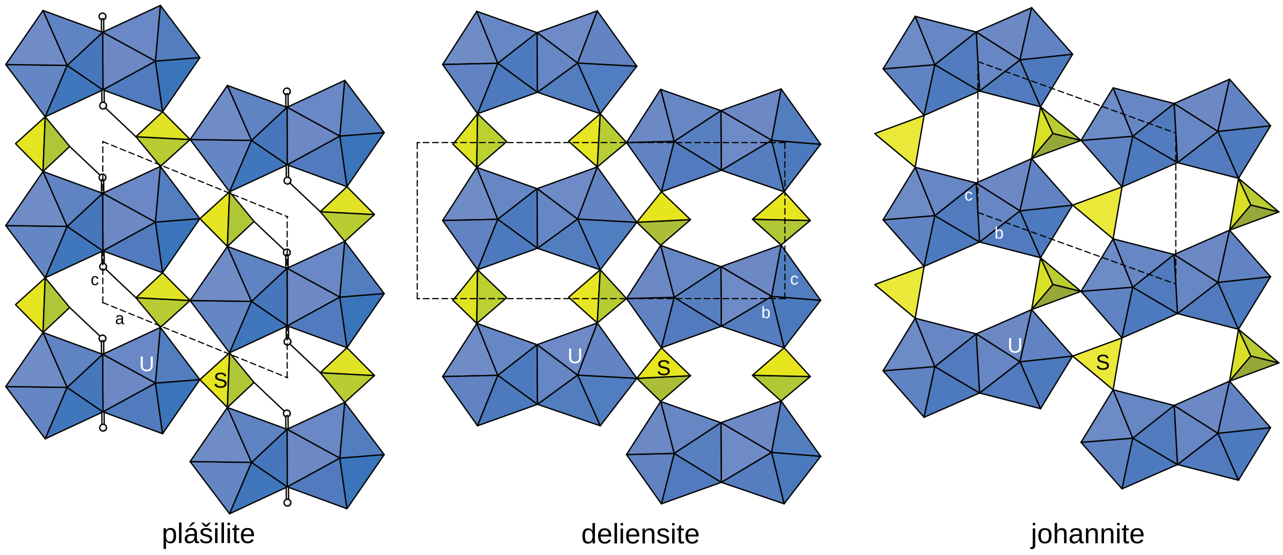

plášilite deliensite johannite

Fig. 5 Sheets in the structures of plášilite, deliensite and johannite. The unit is cell shown by dashed lines. For plášilite, H atoms are represented by white spheres. O–H bonds are drawn as sticks.

Tab. 7 Bond-valence analysis for plášilite (in valence units)

	O1	O2	O3	O4	O5	O6	OH7	OW8	OW9	Σ_c
U		0.46	0.52	0.46	1.69	1.68	0.61, 0.58			5.99
Na	0.18					0.15		0.17, 0.16	0.18, 0.16	1.00
S	1.57	1.47	1.46	1.43						5.93
H7	0.10						0.90			1.00
H8a					0.08			0.92		1.00
H8b							0.07	0.93		1.00
H9a				0.07					0.93	1.00
H9b		0.06							0.94	1.00
Σ_a	1.86	1.99	1.97	1.96	1.77	1.83	2.15	2.18	2.21	

Bond strengths are as follows:

*S^{6+}–O from Brown and Altermatt (1985); Na^{+}–O from Wood and Palenik (1999); U^{6+}–O from Burns et al. (1997); hydrogen based on H···O bond lengths from Brown and Altermatt (1985).

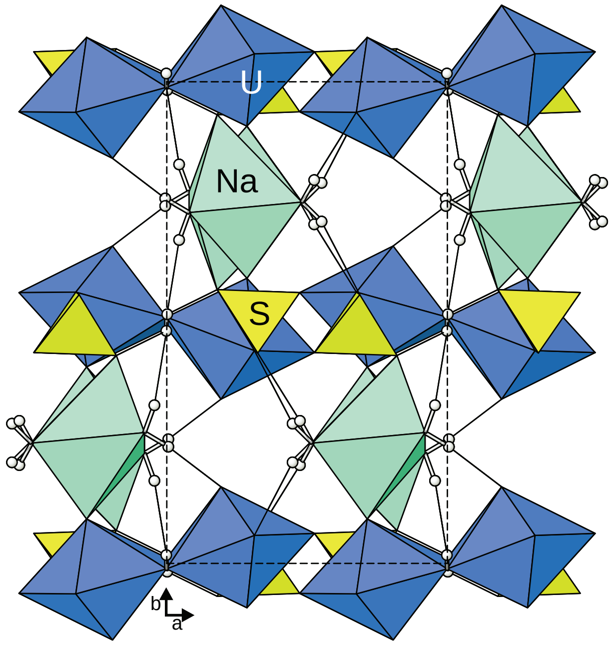

Fig. 6 The crystal structure of plášilite. The unit is cell indicated by dashed lines. Hydrogen atoms are shown as white spheres; O–H bonds are drawn as sticks. Hydrogen bonds are shown as thin lines. Note the chains of $[NaO_2(H_2O)_4]$ octahedra running along [001].

others under study) have structures that contain uranyl dimers.

Acknowledgements. Reviewer Stuart Mills, an anonymous reviewer and handling editor František Laufek are thanked for their constructive comments on the manuscript. Ken Krahulec of the Utah Geological Survey is thanked for providing information about the genesis of the U deposits in the area. The recording of the plášilite Raman spectrum by Ladislav Lapčák (Institute of Chemical Technology, Prague) is highly appreciated. A portion of this study was funded by the John Jago Trelawney Endowment to the Mineral Sciences Department of the Natural History Museum of Los Angeles County. Further support was provided by long-term project DKRVO

2014/02 of the Ministry of Culture of the Czech Republic (National Museum 000232782) to J. Č.

Electronic supplementary material. Supplementary crystallographic data for this paper are available online at the Journal web site (*http://dx.doi.org/10.3190/jgeosci. 184*).

References

Bartlett JR, Cooney RP (1989) On the determination of uranium–oxygen bond lengths in dioxouranium(VI) compounds by Raman spectroscopy. J Mol Struct 193: 295–300

Brown ID, Altermatt D (1985) Bond-valence parameters obtained from a systematic analysis of the inorganic crystal structure database. Acta Cryst B41: 244–248

Burla MC, Caliandro R, Camalli M, Carrozzini B, Cascarano GL, De Caro L, Giacovazzo C, Polidori G, Spagna R (2005) SIR2004: an improved tool for crystal structure determination and refinement. J Appl Cryst 38: 381–388

Burns PC (2005) U^{6+} minerals and inorganic compounds: insights into an expanded structural hierarchy of crystal structures. Canad Mineral 43: 1839–1894

Burns PC, Ewing RC, Hawthorne, FC (1997) The crystal chemistry of hexavalent uranium: polyhedron geometries, bond-valence parameters, and polymerization of polyhedra. Canad Mineral 35: 1551–1570

Chenoweth WL (1993) The Geology and Production History of the Uranium Deposits in the White Canyon Mining District, San Juan County, Utah. Utah Geological Survey Miscellaneous Publications 93–3: pp 1–26

Čejka J (1999) Infrared spectroscopy and thermal analysis of the uranyl minerals. In: Burns PC, Ewing RC (eds) Uranium: Mineralogy, Geochemistry and the Environment. Mineralogical Society of America and Geochemical Society Reviews in Mineralogy and Geochemistry 38: pp 521–622

Čejka J (2004) Vibrational spectroscopy of uranyl minerals – infrared and Raman spectra of uranyl minerals. I. Uranyl, UO_2^{2+}. Bull mineral–petrolog Odd Nár Muz (Praha) 12: 44–51 (in Czech)

Čejka J (2007) Vibrational spectroscopy of uranyl minerals – infrared and Raman spectra of uranyl minerals. III. Uranyl sulfates. Bull mineral–petrolog Odd Nár Muz (Praha) 14–15: 40–46 (in Czech)

Finch RJ, Murakami T (1999) Systematics and paragenesis of uranium minerals. In: Burns PC, Ewing RC (eds) Uranium: Mineralogy, Geochemistry and the Environment. Mineralogical Society of America and Geochemical Society Reviews in Mineralogy and Geochemistry 38: pp 91–179

Frondel C, Ito J, Honea RM, Weeks AM (1976) Mineralogy of the Zippeite Group. Canad Mineral 14: 429–436

Kampf AR, Plášil J, Kasatkin AV, Marty J (2014) Belakovskiite, $Na_7(UO_2)(SO_4)_4(SO_3OH)(H_2O)_3$, a new uranyl sulfate mineral from the Blue Lizard mine, San Juan County, Utah, USA. Mineral Mag 78: 639–649

Higashi T (2001) *ABSCOR*. Rigaku Corporation, Tokyo

Krivovichev SV, Burns PC (2007) Actinide compounds containing hexavalent cations of the VI group elements (S, Se, Mo, Cr, W). In: Krivovichev SV, Burns PC,Tananaev IG (eds) Structural Chemistry of Inorganic Actinide Compounds. Elsevier, Amsterdam, pp 95–182

Krivovichev SV, Plášil J (2013) Mineralogy and Crystallography of Uranium. In: Burns PC, Sigmon GE (eds) Uranium: From Cradle to Grave. Mineralogical Association of Canada Short Courses 43: pp 15–119

Larsen ES (1921) The microscopic determination of the nonopaque minerals. US Geol Surv Bull 679: pp 1–294

Libowitzky E (1999) Correlation of O–H stretching frequencies and O–H···O hydrogen bond lengths in minerals. Monat Chem 130: 1047–1059

Mandarino JA (1976) The Gladstone-Dale relationship – Part I: derivation of new constants. Canad Mineral 14: 498–502

Mandarino JA (1994) Natural and synthetic selenites and selenates and their Gladstone-Dale compatibility. Eur J Mineral 6: 337–349

Mereiter K (1982) Die Kristallstrukturs des Johannits, $Cu(UO_2)_2(OH)_2(SO_4)_2{\cdot}8H_2O$. Tschermaks Mineral Petrol Mitt 30: 47–57

Nakamoto K (1986) Infrared and Raman Spectra of Inorganic and Coordination Compounds. J. Wiley and Sons, New York, pp 1–496

Ondruš P, Veselovský F, Skála R, Císařová I, Hloušek J, Frýda J, Vavřín I, Čejka J, Gabašová A (1997) New naturally occurring phases of secondary origin from Jáchymov (Joachimsthal). J Czech Geol Soc 42: 77–108

Pekov IV, Krivovichev SV, Yapaskurt VO, Chukanov NV, Belakovskiy DI (2014) Beshtauite, $(NH_4)_2(UO_2)(SO_4)_2{\cdot}2H_2O$, a new mineral from Mount Beshtau, Northern Caucasus, Russia. Amer Miner 99: 1783–1787

Piret P, Deliens M (1989) The Gladstone-Dale constant $k(UO_3)$ for uranyl phosphates and arsenates. Canad Mineral 27: 533–534

Plášil J, Hauser J, Petříček V, Meisser N, Mills SJ, Škoda R, Fejfarová K, Čejka J, Sejkora J, Hloušek J, Johannet J.-M, Machovič V, Lapčák L (2012) Crystal structure and formula revision of deliensite, $Fe[(UO_2)_2(SO_4)_2(OH)_2](H_2O)_7$. Mineral Mag 76: 2837–2860

Plášil J, Kampf AR, Kasatkin AV, Marty J, Škoda R, Silva S, Čejka J (2013) Meisserite, $Na_5(UO_2)(SO_4)_3(SO_3OH)(H_2O)$, a new uranyl sulfate mineral from the Blue Lizard mine, San Juan County, Utah, USA. Mineral Mag 77: 2975–2988

Plášil J, Kampf AR, Kasatkin AV, Marty J (2014a) Bluelizardite, $Na_7(UO_2)(SO_4)_4Cl(H_2O)_2$, a new uranyl sulfate mineral from the Blue Lizard mine, San Juan County, Utah, USA. J Geosci 59: 145–158

Plášil J, Veselovský F, Hloušek J, Škoda R, Novák M, Sejkora J, Čejka J, Škácha P, Kasatkin AV (2014b) Mathesiusite, $K_5(UO_2)_4(SO_4)_4(VO_5)(H_2O)_4$, a new uranyl vanadate–sulfate from Jáchymov, Czech Republic. Amer Miner 99: 625–632

Sheldrick GM (2008) A short history of *SHELX*. Acta Cryst A64: 112–122

Tvrdý J, Plášil J (2010) Jáchymov – reiche Erzlagerstätte und Radonbad im böhmischen Westerzgebirge. Aufschluss 61: 277–292

Volod'ko LV, Komyak AI, Umreyko DS (1981) Uranyl Compounds Vol. I, Spectra and Structure. Belorussian State University, Minsk, pp 1–620 (in Russian)

Wood RM, Palenik GJ (1999) Bond valence sums in coordination chemistry. Sodium–oxygen complexes. Inorg Chem 38: 3926–3930